INDIAN JOURNAL OF SCIENCE AND TECHNOLOGY

RESEARCH ARTICLE

OPEN ACCESS

Received: 18-10-2024

Accepted: 11-11-2024

Published: 30-12-2024

Citation: Gayathri P, Xavier A, Ramachandramoorthi PV (2024) Efficient Auramine Yellow Dye Removal using Synthesized Lima Beans Carbon: Kinetic and Isotherm Study. Indian Journal of Science and Technology 17(48): 5099-5106. https://doi.org/10.17485/IJST/v17i48.3442

* **Corresponding author**.

keerthixavi1968@gmail.com

Funding: None

Competing Interests: None

Published By Indian Society for Education and Environment (iSee)

ISSN
Print: 0974-6846
Electronic: 0974-5645

Efficient Auramine Yellow Dye Removal using Synthesized Lima Beans Carbon: Kinetic and Isotherm Study

P Gayathri[1], A Xavier[2]*, P V Ramachandramoorthi[3]

1 Assistant Professor, Department of Chemistry, Sri Adi Chunchanagiri Womens College, Cumbum, 625 516, Tamil Nadu, India
2 Associate Professor and Head, Research Supervisor, PG & Research Department of Chemistry, The Madura College, Madurai, 625 011, Tamil Nadu, India
3 Research Scholar, PG & Research Department of Chemistry, The Madura College, Madurai, 625 011, Tamil Nadu, India

Abstract

Objectives: To evaluate the efficacy of chemically synthesized Lima Beans Carbon (LBC) in removing Auramine Yellow (AY) dye from aqueous solutions through adsorption. **Methods:** LBC was chemically synthesized and characterized using BET isotherm analysis for surface area and pore volume, SEM, EDX, and FTIR for structural insights. Kinetic experiments and various isotherm tests were conducted to validate and evaluate the adsorption process. **Findings:** The LBC adsorbent demonstrated a high adsorption performance for AY dye removal from aqueous solutions. BET isotherm analysis indicated a suitable surface area and pore volume for effective adsorption. Characterization using SEM, EDX, and FTIR confirmed the structural capacity of LBC for dye absorption. Kinetic experiments validated the adsorption nature, and isotherm tests comprehensively evaluated the adsorption process, confirming LBC's high efficiency. **Novelty:** Utilizing Lima Beans Carbon for effective Auramine Yellow dye removal from water.

Keywords: Adsorption; Lima Beans Carbon; Auramine Yellow dye; Adsorption Isotherm; Kinetic studies

1 Introduction

All living things that depend on clean water are seriously threatened by water pollution, which is still an issue from earlier periods. People and animals may be harmed by changes in water's physical and chemical characteristics [1]. Water pollution occurs when harmful substances, including chemicals, waste, and toxic materials, enter water bodies, degrading the water quality and making it unsafe for use. Pollutants can come from various sources, such as industrial discharge, agricultural runoff, sewage, and urban waste. Heavy metals are metallic elements with high densities, atomic weights, or atomic numbers. When they enter water systems, they pose severe risks due to their toxicity, persistence, and bioaccumulative nature. Unlike organic pollutants, heavy metals do not degrade in the environment and can accumulate in the tissues of living organisms, magnifying in concentration as they move up the food chain. Industrial effluents from large-scale production and rapid industrial expansion have resulted in the widespread use of clean water for manufacturing and cleaning, which has led to the release of numerous contaminants into natural water bodies, including bacteria, heavy metals, dyes, and non-degradable components[2]. Innovative and economical treatment methods are becoming increasingly necessary to solve this problem[3]. Adsorption is a popular technology for treating primary water contaminants because of its effectiveness and the benefit of not creating secondary sludge, among its many other benefits. This research uses Lima Beans Carbon (LBC) powder-activated carbon to remove Auramine Yellow (AY) dye from the water. Lima beans play a role in sequestering and emitting carbon through their growth and cultivation. By implementing sustainable agricultural practices, their positive impact on carbon sequestration can be maximized, contributing to efforts to mitigate climate change. Therefore, it was determined that this substance should be utilized to eliminate the AY dyes from the water. Batch mode of adsorption studies was carried out and several characterization techniques were used to assess the generated adsorbent material's performance.

2 Materials and method

2.1 AY and LBC preparation

In one liter of distilled water, 100 mg of Auramine Yellow dye was dissolved to produce a concentration of 100 mg/L, which was then used to set up the stock solution. Following up to ten hours of sun drying, the sample was heated to 200°C for twenty-four hours in a muffle furnace. Before being used for batch experimental investigations, the adsorbent material was first heated to 80°C in an oven.

2.2 Characterization of LBC

At -196°C, nitrogen adsorption was used to measure the surface area of LBC. Using Brunauer-Emmett-Teller (BET) analysis, the surface area of the activated adsorbent was determined after it was heated to 300°C for five hours to eliminate gas molecules. With a 4 cm^{-1} interval and 20 scans, FTIR analysis was carried out between 400 and 4000 cm^{-1}. Pollutant presence on the adsorbent surface was confirmed by scanning electron microscopy (SEM), and targeted pollutant adsorption on the LBC surface was validated by energy dispersive X-ray (EDX) analysis.

2.3 Isotherm and Kinetic Studies

2.3.1 Langmuir and Freundlich isotherm

Based on the supposition that chemical processes mediate the binding mechanism between AY dye and LBC adsorbent, the study explains the adsorption changes process. Equation (1) is the linear equation that represents this isotherm investigation. The Freundlich model is used to describe the adsorption of solutes from a liquid onto a solid surface. It is particularly useful for characterizing adsorption processes where the adsorption capacity is not uniform across the surface, which is often the case with heterogeneous surfaces. Equation (2) expresses the linear form of this model.

$$\frac{C_e}{q_e} = \frac{1}{K.q_{max}} + \frac{C_e}{q_{max}} \tag{1}$$

$$Lnq_e = lnk_f + \frac{1}{n} lnC_e \tag{2}$$

2.3.2 Pseudo-first-order and Pseudo-second-order studies

A solid adsorption capacity was determined and assessed using this model in the context of solid and liquid systems. According to this concept, the driving force and the metal ion desorption are exactly related. Equation (3) expresses the linear form of this model. The effectiveness of the AY dye removal process has been evaluated using the pseudo-second-order study, predicated on the idea that the quantity of copper ions adsorbed is directly proportional to the active site availability in activated sawdust charcoal adsorbent. Equation (4) may be used to define the equation for this model.

$$log(q_e - q) = logq_e - \frac{k}{2.303} t \tag{3}$$

$$\frac{t}{q} = \frac{1}{h} + \frac{1}{q_e} t \tag{4}$$

3 Results and Discussion

3.1 Batch adsorption studies

3.1.1 Impact of pH and adsorbent dose

For 60 minutes at 30°C, 1 g/L of LBC was added to a solution containing 20 mg/L of AY dye in the first experiment. A pH range of 2.0 to 7.0 was used to test the effectiveness of metal ion adsorption. As seen in Figure 1 **a**, the largest quantity of AY dye was found to adsorb efficiently at very low pH conditions. Metal ions from the synthetic solution adsorb less readily when pH rises. The adsorption rate can be increased at low pH levels by the efficient reaction of positively charged ions with negatively charged particles[(4)]. In particular, it was shown that, in this batch sample, about 65% of the AY dye concentration was adsorbed at an ideal pH of 2.0.

With 0.1 to 1 g/L of LBC dose adjustment, the experiment was conducted with the ideal pH set to 2.0, 20mg/L of AY concentration, and contact time of 1 hour at 25°C. The effect of AY dye absorption is seen by changing the adsorbent dosage in Figure 1**b**. When the adsorbent reached a dosage of 0.6 g/L, there was an abrupt drop in the dye absorption that had previously been rapid. Pollutants from the aqueous solutions are taken up more readily by the adsorbent at greater dosages because there are more active sites available. At the ideal dosage of 0.6 g/L, around 65.05% of the AY dye was eliminated. Beyond this point, the concentration gradient plateaued or decreased at higher dose levels, resulting in reduced AY dye uptake[(5)].

3.1.2 Impact of varying the dye concentration and contact time

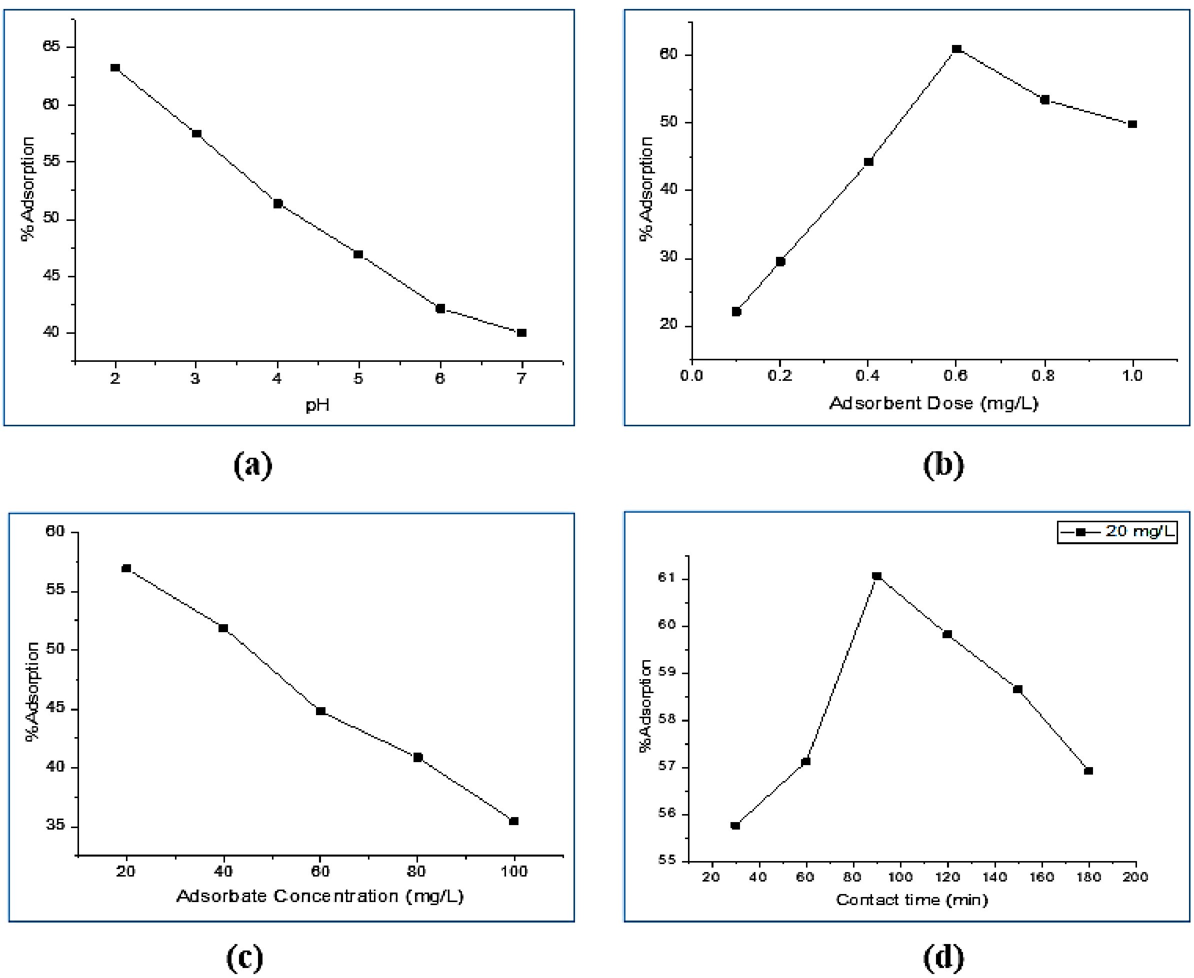

Fig 1. Impact of AY uptake (a) pH, (b) adsorbent dose, (c) initial concentration, (d) contact time

This experiment examined the effect of AY dye absorption by LBC adsorbent, with the AY dye concentration in synthetic solutions varied from 20 to 100 mg/L, 1 hour of reaction time at 30°C. The ideal pH for the investigation was 2.0, and the LBC concentration was 0.6 g/L. By altering the dye concentrations in aqueous solutions, Figure 1**c** shows the effects of AY adsorption. It was shown that at lower AY dye solution concentrations, the most adsorption happened. This is probably because the adsorption capability of LBC is limited at greater dye concentrations because of the reduced accessibility of dynamic places in LBC [6].

The investigation was carried out at an optimal pH of 2.0, 20 mg/L of AY dye level, and LBC concentration of 0.6 g/L in the experiment where the contact duration between AY dye solution and LBC adsorbent was varied from 10 to 180 minutes. The changes in adsorption efficiency about contact time are shown in Figure 1**d**. The active sites in the LBC were high, and the dye absorption was initially fast [7]. There were fewer available sites for further adsorption as a consequence of the contaminants that gradually occupied these active sites over time. As a result, as the image illustrates, the effectiveness of AY dye absorption declined after 90 minutes [8].

Adsorbent Characterization

A thorough view of LBC is shown in Figure 2**a** and **b**, which show images taken at different working distances of 10 μm and 5 μm before and after auramine yellow uptake. The adsorbent surface in Figure 2**a** first shows a lot of active sites and irregular pores, both of which are good for adsorbing contaminants from aqueous media. These energetic spots and openings are packed with pollutants after being exposed to an auramine yellow solution, as seen by the SEM picture in Figure 2**b**, which makes a layer visible on the surface of the adsorbent. When saturation was reached—as evidenced by the absence of additional adsorption changes the procedure was finished [9]. Analogously to SEM examination, auramine yellow was adsorbed using LBC adsorbent, and EDX analysis was carried out both before and after. The EDX pictures of the biochar adsorbent before and after auramine yellow adsorption are shown in Figure 2**c** and **d**. The surface of the biochar displayed a variety of chemical and metallic constituents, most notably carbon in large numbers, as well as oxygen, calcium, and other elements [10]. After saturation with the synthetic solution, an EDX picture (Figure 2 **b**) verified that auramine yellow had been adsorbed on LBC, viewing the occurrence of aluminium, potassium, and chromium in addition to carbon and oxygen [11].

To determine the functional groups that were present in the LBC adsorbent, FTIR analysis was performed. As shown in Figure 2**e** and **f**, evaluations were conducted on charcoal adsorbents that had been activated chemically as well as naturally. Carbonyl group ring vibrations are responsible for the raw adsorbent's noticeable peak in Figure 2**a**, which was seen at 1602 cm^{-1} [12]. The largest peak in Figure 2**f**, which was caused by symmetrical bending, showed stretching vibrations of O-H groups at 2924 cm^{-1}. Furthermore, a peak at 1595 cm^{-1} revealed bending vibrations of CH_2, and a wide band extending to 3390 cm^{-1} suggested the existence of water and alcohol functional groups with different stretching vibrations [13]. The fact that peaks start to fade at 1092 cm^{-1} indicates that -COO stretching occurred. At 40 kV and 250 mA, CuK-α radiation was used in X-ray Diffraction (XRD) examination to examine the crystalline structure of the adsorbent material. For the raw and activated LBC adsorbents, respectively, the XRD peaks are shown in Figure 2 **g** and **h**. The activated LBC charcoal showed substantial improvements in intensity and crystalline structure as compared to the raw adsorbent [14]. A good match was found between the activated LBC charcoal's XRD pattern and peaks at 2θ values that corresponded to 160, 240, 280, 311, 395, and 480, or 80, 110, 60, 40, 35, and 20 hkl planes, as appropriate. Its structural properties and crystallinity are confirmed by these measurements, which show a crystalline nature for the adsorbent material with high intensities [15].

Isotherm studies

The linear plots of this isothermal study are shown in Figure 2 **a**, and the process of dye removal has been examined by monolayer or multilayer process using this study. The values of this isothermal model were intended from the linear plots and the values of each constant were listed in Table 1. Referring to the table, the separation parameter value is 0.38, which is in the range between 0 to 1 and may confirm the favorable adsorption process [16]. Also, higher regression values (R^2) indicate the applicability of the isothermal model.

The process of heterogeneity was assessed using this isothermal study based on the linear plots. The Freundlich isotherm study's linear plot, which yielded the values for the slope and intercept, is displayed in Figure 2**b**. Both the adsorption capacity and adsorption intensity were computed using these values. Table 1 lists the 30°C values of the Freundlich isotherm constants. A value of 3.125 for the adsorption capacity was discovered, falling between 0 and 1. It is also confirmed that the Freundlich isotherm model is applicable by the regression value being larger than 0.95. So, the LBC adsorbent's absorption of auramine yellow is heterogeneous and involves multilayer adsorption.

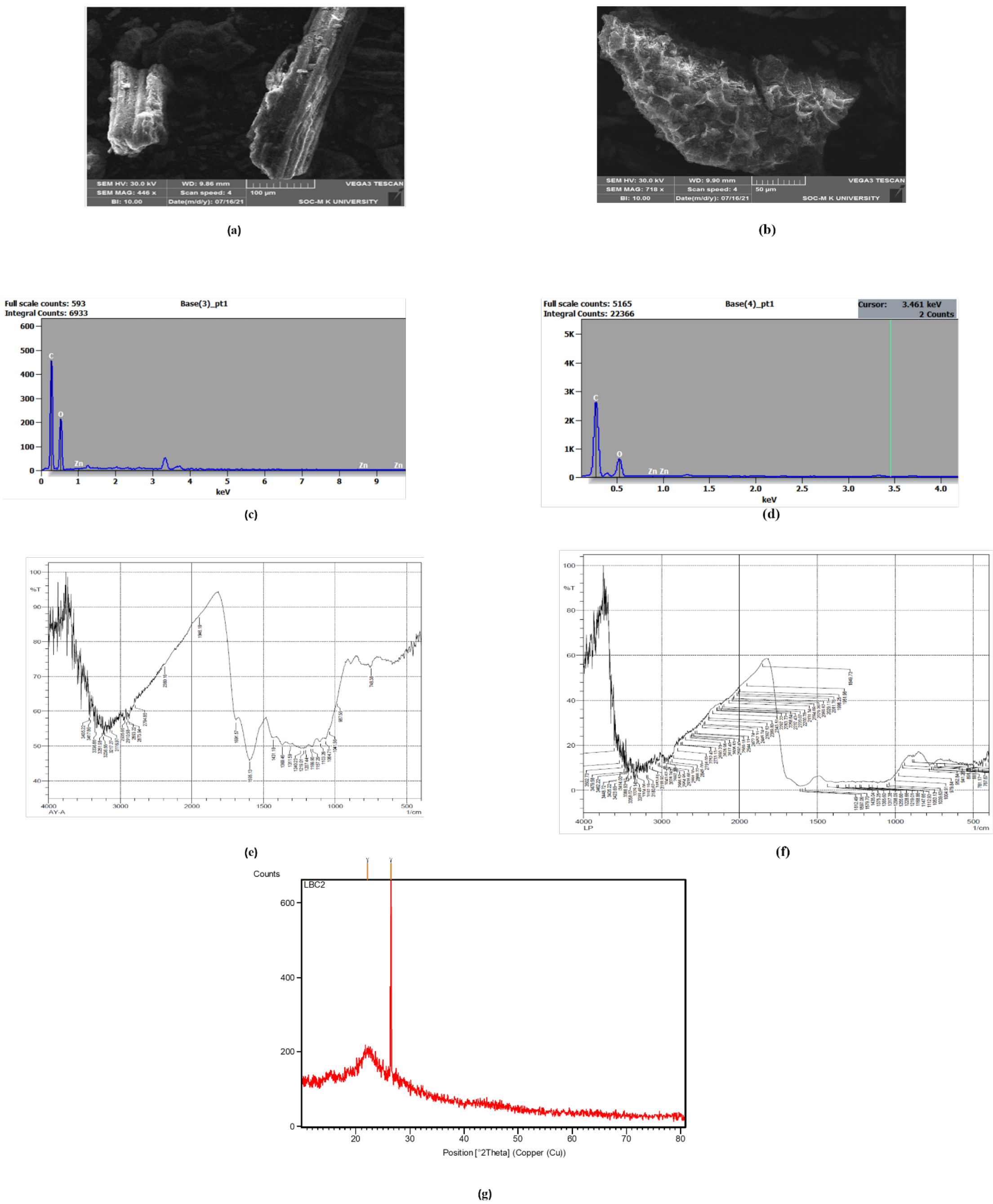

Fig 2. Characterization of LBC (a, b) SEM, (c, d) EDAX, (e, f) FTIR, (g) XRD

Table 1. Constants of various isotherm models for AY adsorption

S. No.	Model	Parameters	Isotherm constants
1.	Langmuir	q_{max}	10.283
		R_L	0.381
		R^2	0.9704
2.	Freundlich	K_f	2.831
		n	2.621
		R^2	0.992

Kinetic studies

Linear graphs of (qe - q) vs (t), as shown in Figure 2 **c**, were used to evaluate the kinetics of Auramine yellow adsorption by LBC adsorbent. The model variables were calculated and they are shown in Table 2. These plots' kinetic rate constants (k) and regression values (R^2) show that they match well with the adsorption process. The applicability of the model in chromium adsorption is confirmed by the linear plot's regression value, which is more than 0.95. Regression analysis also showed that the adsorption process had achieved equilibrium [17].

As seen in Figure 2**d**, linear plots of (t/q) vs (t) were used to investigate the second-order kinetics. The different constants of this kinetic model are displayed in Table 2, where a high regression value is noted. The values of (qe) computed using the linear equations were in good agreement with the results acquired via experimentation. These results demonstrated that the second-order kinetics matched the adsorption process effectively, pointing to the adsorption saturation point inside the system's bounds [18].

Adsorption thermodynamics

Figure 3 showed different dye concentrations from 20 – 100 mg/L, along with the thermodynamic study of AY dye adsorption using LBC. The thermodynamic constants were calculated from the plot and listed in Table 3. It was discovered that the enthalpy change (ΔHo) values were positive, signifying that the process of AY dye adsorption onto LBC is endothermic [19]. Nonetheless, the adsorption appears to be spontaneous under the investigated conditions, based on the negative values of the Gibbs free energy change (ΔGo). Moreover, throughout the AY dye adsorption process with LBC adsorbent, Table 3's positive entropy change (ΔSo) results show a rise in the disorderliness of the solid and liquid phases [20].

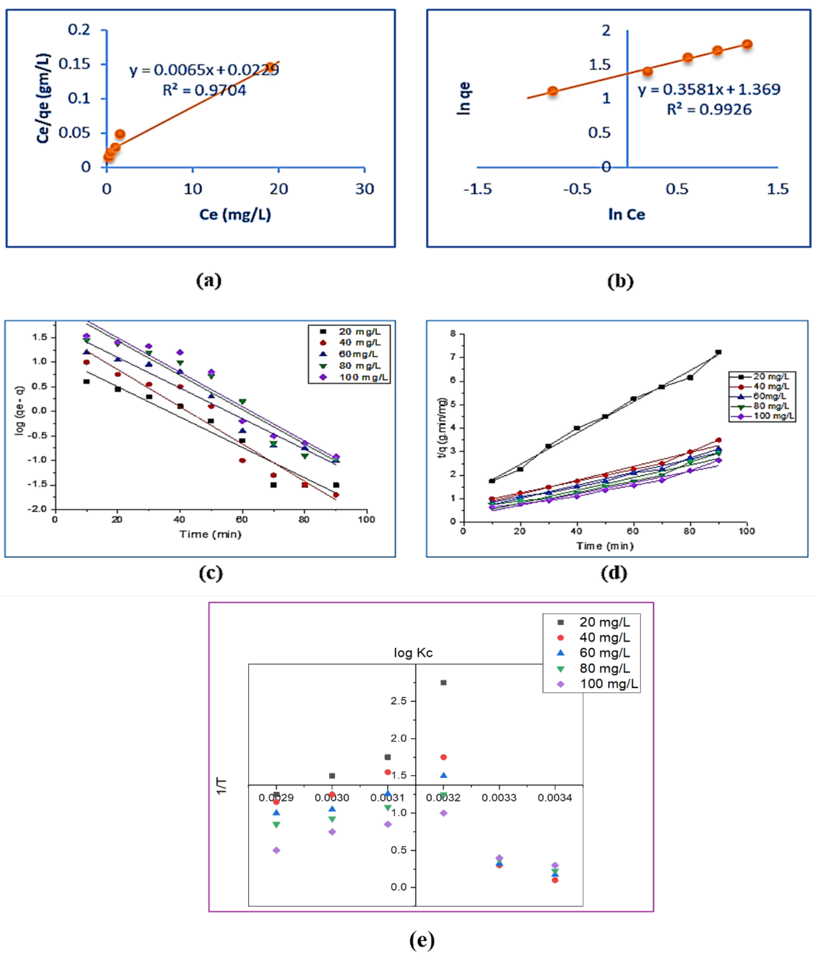

Fig 3. (a, b) Langmuir and Freundlich Isotherm, (c, d) PFO and PSO Kinetics, (e) Thermodynamic plots

Table 2. Adsorption kinetic constants for AY removal using LBC

S. No.	AY dye level	PFO			PSO			
		K(min^{-1})	q_e, cal (mg/g)	R^2	K (g/mg.min) X 10^{-3}	q_e, cal (mg/g)	h (mg/g.min)	R^2
1.	20	0.041	3.21	0.95	21.41	5.13	0.15	0.97
2.	40	0.059	7.04	0.96	19.38	9.48	0.17	0.95
3.	60	0.072	10.23	0.97	13.53	10.64	0.24	0.97
4.	80	0.063	13.82	0.96	10.49	13.84	0.27	0.95
5.	100	0.051	17.38	0.95	8.18	19.53	0.34	0.96

Table 3. Adsorption thermodynamics of AY removal using LBC

Level of AY dye concentration	ΔH_o KJ mol^{-1}	ΔS_o J mol^{-1}	Gibbs Energy (ΔG_o) kJ mol^{-1}			
			20°C	40°C	60°C	80°C
20	72.297	162.765	-15.201	-11.634	-9.853	-7.285
40	39.462	89.479	-11.592	-9.482	-7.034	-6.384
60	18.446	41.831	-9.293	-6.349	-5.895	-4.895
80	11.756	29.761	-6.353	-4.839	-3.473	-3.027
100	8.592	21.162	-4.685	-3.253	-2.845	-2.348

Desorption studies

Concentrated sulfuric acid was used in desorption experiments to recover the AY dye absorbed by LBC at different concentrations between 0.1 N and 0.4 N. It was found that the recovery of AY dye was remarkably effective, especially with when increase in acid concentration [21,22]. Above this dose, the reduction rate was decreased slowly. When 0.3 N H_2SO_4 was added, AY dye recovery reached a saturation point; when equilibrium was attained, there was no further rise in ion regaining [23–25]. In particular, 93.27% of AY was recovered from the used adsorbent in our experimental investigation using 0.3 N H_2SO_4 acid. Later, the recovered AY dye was used in additional experimental research.

4 Conclusion

Lima Bean Carbon (LBC) adsorbent was used to study the biosorption of auramine yellow (AY) dye from synthetic solutions. LBC eliminated 65% of the AY dye concentration when the ideal parameters were met, which included pH 2.0, 0.6 g/L of adsorbent dosage, and a 90-minute contact period. Both the Langmuir and Freundlich model isotherms were followed by the adsorption process, suggesting heterogeneous monolayer/multilayer adsorption. Furthermore, LBC's absorption of AY dye followed both PFO and PSO models. Positive and negative numbers from thermodynamic analysis indicated that there was some degree of uncertainty in the interactions between the solid and liquid during the adsorption process. Strong sulfuric acid was employed to desorb the AY dye.

Financial Disclosure/Conflict of Interest

The authors declare that there was no financial aid received and no conflict of interest associated with this research work.

References

1) Priya AK, Yogeshwaran V, Rajendran S, Hoang TKA, Soto-Moscoso M, Ghfar AA, et al. Investigation of mechanism of heavy metals (Cr6+, Pb2+ & Zn2+) adsorption from aqueous medium using rice husk ash: Kinetic and thermodynamic approach. *Chemosphere*. 2022;286. Available from: https://doi.org/10.1016/j.chemosphere.2021.131796.
2) Pholosi A, Naidoo EB, Ofomaja AE. Intraparticle diffusion of Cr (VI) through biomass and magnetite coated biomass: A comparative kinetic and diffusion study. *South African Journal of Chemical Engineering*. 2020;32:39–55. Available from: https://doi.org/10.1016/j.sajce.2020.01.005.
3) Halim AA, El-Ezaby KH, El-Gammal MI, Saber HM. Removal of Fe2+ and Pb2+ ions from wastewater using rice husk based adsorbents. *Journal of Egypt Academy of Society and Environmental Development*. 2019;20:47–60. Available from: https://jades.journals.ekb.eg/article_67694_c3d67c52c85b11da6dd98d1d4979e141.pdf.

4) Brinza L, Maftei AE, Tascu S, Brînză F, Neamtu M. Advanced removal of Reactive Yellow 84 azo dye using functionalized amorphous calcium carbonates as adsorbent. *Scientific Reports*. 2022;12. Available from: https://www.nature.com/articles/s41598-022-07134-2.
5) Sheeja J, Sampath K, Kesavasamy R. Experimental investigations on adsorption of reactive toxic dyes using Hedyotis umbellate activated carbon. *Adsorption Science and Technology*. 2021;2021:1–12. Available from: https://doi.org/10.1155/2021/5035539.
6) Saeed MM, Ahmed M. Effect of temperature on kinetics and adsorption profile of endothermic chemisorption process: -Tm (III)-PAN loaded PUF system. *Separation Science and Technology*. 2007;41(4):705–722. Available from: https://doi.org/10.1080/01496390500527993.
7) Ziarati P, Far BF, Mashayekhi E, Sawicka B. Removing arsenic by food processing waste (Ziziphus jujuba seeds) and study on its adsorption properties. *Scientific and Technical Journal Technogenic and Ecological Safety*. 2019;5:62–70. Available from: https://www.researchgate.net/publication/331981897_Scientific_and_technical_journal_Technogenic_and_Ecological_Safety_REMOVING_ARSENIC_BY_FOOD-PROCESSING_WASTE_ZIZYPHUS_JUJUBA_SEEDS_AND_STUDY_ON_ITS_ADSORPTIVE_PROPERTIES.
8) Khan TA, Noumana M, Dua D, Khan SA, Alharthi SS. Adsorptive scavenging of cationic dyes from aquatic phase by H3PO4 activated Indian jujube (Ziziphus mauritiana) seeds based activated carbon: Isotherm, kinetics, and thermodynamic study. *Journal of Saudi Chemical Society*. 2022;26(2):1–16. Available from: https://doi.org/10.1016/j.jscs.2021.101417.
9) Yogeshwaran V, Priya AK. Experimental studies on the removal of heavy metal ion concentration using sugarcane bagasse in batch adsorption process. *Desalination and Water Treatment*. 2021;224:256–272. Available from: https://www.deswater.com/DWT_articles/vol_224_papers/224_2021_256.pdf.
10) Chakraborty S, Mukherjee A, Das S, Maddel NR, Iram S, Das P. Study on isotherm, kinetics, and thermodynamics of adsorption of crystal violet dye by calcium oxide modified fly ash. *Environmental Engineering Research*. 2021;26(1). Available from: https://doi.org/10.4491/eer.2019.372.
11) Gajipara YN, Balpande DN, Patil PS, Yadav AA, Yadav MD, Patwardhan AV. Jackfruit Leaf-Based Natural Adsorbent for the Efficient Removal of Auramine O Dye. *Water Conservation Science and Engineering*. 2023;8. Available from: https://link.springer.com/article/10.1007/s41101-023-00209-9.
12) Kerrou M, Bouslamti N, Raada A, Elanssari A, Mrani D, Slimani MS. The use of sugarcane bagasse to remove the organic dyes from wastewater. *International Journal of Analytical Chemistry*. 2021;2021:1–11. Available from: https://doi.org/10.1155/2021/5570806.
13) El-Nemr MA, Yılmaz M, Ragab S, Hassaan MA, Nemr AE. Isotherm, and kinetic studies of acid yellow 11 dye adsorption from wastewater using Pisum Sativum peels microporous activated carbon. *Scientific Reports*. 2023;13. Available from: https://www.nature.com/articles/s41598-023-31433-x.
14) Nur JW, Lim MR, Bilad AH, Mahadi J, Hobley A, Usman. 2023. Available from: https://doi.org/10.1016/j.emcon.2022.100199.
15) Yu J, Zhu J, Feng L, Cai X, Zhang Y, Chi R. Removal of cationic dyes by modified waste biosorbent under continuous model: Competitive adsorption and kinetics. *Arabian Journal of Chemistry*. 2019;12(8):2044–2051. Available from: https://doi.org/10.1016/j.arabjc.2014.12.022.
16) Rápó E, Tonk S. Factors Affecting Synthetic Dye Adsorption; Desorption Studies: A Review of Results from the Last Five Years (2017-2021). *Molecules*. 2021;26(17). Available from: https://doi.org/10.3390/molecules26175419.
17) Shindhal T, Rakholiya P, Varjani S, Pandey A, Ngo HH, Guo W, et al. A critical review on advances in the practices and perspectives for the treatment of dye industry wastewater. *Bioengineered*. 2021;12(1):70–87. Available from: https://doi.org/10.1080/21655979.2020.1863034.
18) Lu YC, Priyantha N, Lim LBL, Suklueng M. Toxic yellow cow dung powder (Auramine O dye) removal via Ipomoea aquatica waste. *Desalination and Water Treatment*. 2020;181:422–435. Available from: https://doi.org/10.5004/dwt.2020.25118.
19) Khan TA, Nouman M, Dua D, Khan SA, Alharthi SS. Adsorptive scavenging of cationic dyes from aquatic phase by H3PO4 activated Indian jujube (Ziziphus mauritiana) seeds based activated carbon: Isotherm, kinetics, and thermodynamic study. *Journal of Saudi Chemical Society*. 2022;26(2). Available from: https://dx.doi.org/10.1016/j.jscs.2021.101417.
20) Sheeja J, Sampath K, Kesavasamy R. Experimental Investigations on Adsorption of Reactive Toxic Dyes Using Hedyotis umbellate Activated Carbon. *Adsorption Science & Technology*. 2021;2021:1–12. Available from: https://dx.doi.org/10.1155/2021/5035539.
21) Ambaye TG, Vaccari M, van Hullebusch ED, Amrane A, Rtimi S. Mechanisms and adsorption capacities of biochar for the removal of organic and inorganic pollutants from industrial wastewater. *International Journal of Environmental Science and Technology*. 2021;18(10):3273–3294. Available from: https://dx.doi.org/10.1007/s13762-020-03060-w.
22) Benjelloun M, Miyah Y, Evrendilek GA, Lairini FZS. Recent Advances in Adsorption Kinetic Models: Their Application to Dye Types. *Arabian Journal of Chemistry*. 2021;14(4):1–24. Available from: https://doi.org/10.1016/j.arabjc.2021.103031.
23) Sellaoui L, Gómez-Avilés A, Dhaouadi F, Bedia J, Bonilla-Petriciolet A, Rtimi S, et al. Adsorption of emerging pollutants on lignin-based activated carbon: Analysis of adsorption mechanism via characterization, kinetics and equilibrium studies. *Chemical Engineering Journal*. 2023;452(2). Available from: https://dx.doi.org/10.1016/j.cej.2022.139399.
24) Dhaouadi F, Sellaoui L, Taamalli S, Louis F, Bakali AE, Badawi M, et al. Enhanced adsorption of ketoprofen and 2,4-dichlorophenoxyactic acid on Physalis peruviana fruit residue functionalized with H2SO4: Adsorption properties and statistical physics modeling. *Chemical Engineering Journal*. 2022;445. Available from: https://doi.org/10.1016/j.cej.2022.136773.
25) Edet UA, and AOI. Kinetics, Isotherms, and Thermodynamic Modeling of the Adsorption of Phosphates from Model Wastewater Using Recycled Brick Waste. *Processes* . 2020;8(6):1–15. Available from: https://doi.org/10.3390/pr8060665.